LEVITATION OF CORE FLOWS

C. MATA, R. BAI & D. D. JOSEPH
University of Minnesota
Department of Aerospace Engineering and Mechanics
107 Akerman Hall, 110 Union Street
Minneapolis, MN 55455, USA

Abstract

A simple model is proposed for a 2D horizontal core annular flow in which the effect of gravity due to the difference in the densities of the two fluids is the eccentricity of the core. We split the domain through the center of the core; we characterized each sub domain by means of local variables, for instance the holdup ratio. We found that the smallest global pressure drop is achieved if and only if the local holdup ratios are equal to the global holdup ratio (for a perfect core annular flow this only happens when the core is centered). We used this result in a direct simulation of spatially periodic 2D wavy core annular flows carried out under the assumption that the viscosity of the oil core is so large that it moves as a rigid solid which may nevertheless be deformed by pressure forces in the water. The waves that develop are asymmetric with steep slopes in the high pressure region at the front face of the wave crest and shallower slopes at the low pressure region at lee side of the crest, as Bai et al. describe (1996). However two new issues are confronted in our 2D simulation. First, the shape and length of the upper and lower waves are different. Second, the displaced 2D core can be thought to represent eccentricity. We conclude that a positive pressure force is required to levitate the core off the wall when the densities are not matched and that the difference in the upper and lower wave shapes restore the effect of the eccentricity by allowing the local holdup ratios to be equal to the global holdup ratio; thus the pressure drop is the smallest possible.

1. Introduction

Lubricated pipelining of viscous materials like heavy crude, slurries and capsules is robustly stable and has a high economic potential. The viscous material does not touch the wall. After Joseph and Renardy (1993) the drag reduction in the case of crude oil, which can be achieved by lubrication is of the order of the viscosity ratio with increased throughputs of ten thousand or more. These lubricated flows are called core flows because the viscous material flows in a core lubricated all around by water.

A surprising property of core flows is that the flow in a horizontal line will lubricate with the core lubricated off the wall even if the core is lighter or heavier than the lubricating water. This levitation could not take place without a hydrodynamic lifting action due to waves sculpted on the core surface. In the case of very viscous liquids, the waves are basically standing waves which are convected with the core as it moves downstream. This picture suggests a lubrication mechanism for the levitation of the core analogous to mechanisms which levitate loaded sliders leavings at low Reynolds numbers. Ooms et al.

H. Ramkissoon (ed.), IUTAM Symposium on Lubricated Transport of Viscous Materials, 65-84

[1984] and Oliemans and Ooms (1986) gave a semi empirical model of this type and showed that it generated buoyant forces proportional to the first power of the velocity to balance gravity.

Feng, Huang and Joseph (1995) suggested that the conventional mechanism of lubrication can not describe the water lubricated pipelining of crude oil. They predicted that the high pressures on the forward facing slope of the wave, where the water enters into a converging gap, steepens the wave and the low pressure on the lee side smoothes the wave there. This leads to unsymmetric waves which are actually nearly opposite to the ones which are necessary to levitate a slipper bearing. They also predicted the existence a threshold Reynolds number corresponding to a change in the sign of the pressure force on the core, from suction at Reynolds number below the threshold, as in the reversed slipper bearing in which the slipper is sucked to the wall, to compression for Reynolds number greater than the threshold as in flying core flow in which the core can be pushed off the wall by stagnation pressure.

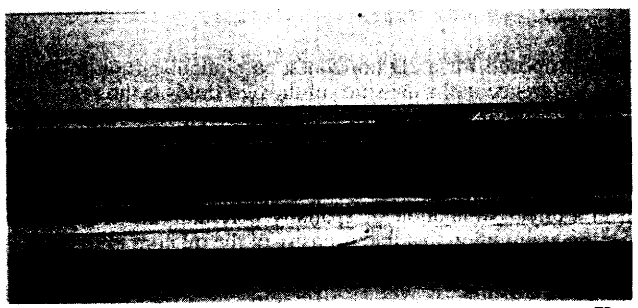

Figure 1.1 Wavy core annular flow in a 1" diameter glass pipe for Reynolds number $\Re$=533, oil to water volume ratio η=0.9 and holdup ratio h=1.4. The upper and lower wave lengths are clearly different.

Figure 1.1 presents a wavy core annular flow in a 1" diameter glass pipe. The wave shape definitely looks like the flying core flow described by Feng et al. (1995). However, the upper and lower wave lengths are clearly different. This difference is due to the buoyancy force acting on the core, because the oil and water densities are not matched. Moreover, the overall effect is an eccentric core flow, which is a 3D problem in a pipe.

Bai, Kelkar and Joseph (1996) performed a direct simulation of interfacial waves in a high viscosity ratio and axisymmetric core annular flow, in which the water and oil densities were matched. In this case the problem of levitation does not arise. However, they computed the pressure distribution that actually develops on the wave and they found that it is such as to levitate a slightly displaced core only when the Reynolds number is greater than a threshold value which depends on the involved parameters. Lubrication by inertia was suggested from this analysis.

The purpose of this work was to carry out a direct simulation of core flows under gravity when the densities are not matched. For simplicity a 2D domain was chosen.

2. 2D perfect core flow

What we call 2D perfect core flow is actually an ideal situation in which two fluids (fluid 1 and fluid 2) with the same density and different viscosities ($\frac{\mu_2}{\mu_1} < 10^{-5}$) flow down an infinite two dimensional horizontal pipeline in a core annular configuration (see figure 2.1), where the interfaces are perfectly smooth and the core is not necessarily centered. We assume that there is a connection somewhere between the upper and lower annuli.

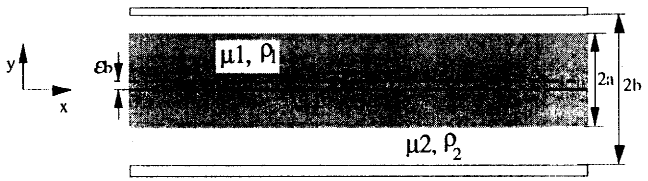

Figure 2.1 Eccentric 2D perfect core flow ($\rho_1=\rho_2$ and $\frac{\mu_2}{\mu_1} < 10^{-5}$). Here ε is a dimensionless measure of the eccentricity.

The pressure field is given by equation (2.1) in the core and, by equation (2.2) in the upper and lower annuli.

$$P_1 = \gamma x - \rho_1 g y + C_1, \tag{2.1}$$

$$P_2 = \gamma x - \rho_2 g y + p(y) + C_2. \tag{2.2}$$

Notice that $\frac{dP_1}{dx} = \frac{dP_2}{dx} = \frac{dP}{dx} = \gamma$ is a unique pressure gradient within the whole domain.

The velocity field in the regions $-b \le y \le -a$ *and* $a \le y \le b$ can be obtained from

$$\frac{\partial u}{\partial x} = 0$$
$$\frac{\partial^2 u}{\partial y^2} = 2\Gamma \tag{2.3}$$

where $\Gamma = -\frac{\gamma}{2\mu_2}$. Since both fluids have the same density, no buoyancy force is present and the position of the core is not fixed.

2.1 SYMMETRIC 2D PERFECT CORE FLOW (PCF)

The solution of equations (2.3) for the symmetric 2D PCAF will be now presented as a function of the geometric parameters shown in figure 2.2, for which the eccentricity ε is

zero, and the pressure gradient $\frac{dP}{dx}=\gamma$. The boundary conditions for the velocity are $u=c,\quad v=0$ in the region $-a\le y\le a$, And $u=c\quad v=0$ at $y=-b\quad y=b$. The shear stress condition at $y=-a$ and $y=a$ is $\mu_1\frac{\partial u}{\partial y}=\mu_2\frac{\partial u}{\partial y}$. Obviously, terms involving the ratio $\frac{\mu_2}{\mu_1}<10^{-5}$ were neglected.

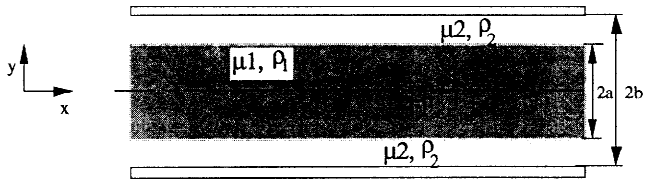

Figure 2.2 Symmetric 2D perfect core flow ($\rho_1=\rho_2$ and $\frac{\mu_2}{\mu_1}<10^{-5}$).

The core velocity c is:

$$c=\Gamma b^2(1-\eta^2) \tag{2.4}$$

where $\eta=\frac{a}{b}$ and $\Gamma=-\frac{\gamma}{2\mu_2}$.

The total flow rate of fluid 1 is:

$$Q_1=2ac=2\Gamma b^3\eta(1-\eta^2) \tag{2.5}$$

The total flow rate Q_2 and average velocity V_2 for fluid 2 are given by equations (2.6) and (2.7), respectively.

$$Q_2=\tfrac{2}{3}\Gamma b^3(2-3\eta+\eta^3) \tag{2.6}$$

$$V_2=\frac{Q_2}{2b(1-\eta)} \tag{2.7}$$

The holdup ratio h, is convenient parameter defined as the ratio of the average velocities of fluid 1 and fluid 2. It can be expressed as follows:

$$h=\frac{c}{V_2}=\frac{3(1-\eta)(1-\eta^2)}{2-3\eta+\eta^3} \tag{2.8}$$

Notice that $\lim_{\eta\to 0}h=1.5$ and $\lim_{\eta\to 1}h=2$. These limits correspond to an ideal core flow. However, this result allows us to set the upper limit of the holdup ratio in a real situation, and this would be between 1.5 and 2.

2.2 ECCENTRIC 2D PERFECT CORE FLOW (PCF)

The solution of equations (2.3), with β instead of γ as the pressure gradient or $\frac{dP}{dx}=\beta$, will be now presented as a function of the geometric parameters shown in figure 2.1, on which the frame of reference is located in the center of the core. The boundary conditions for the velocity are $u=c\quad v=0$ in the region $-a\le y\le a$, And $u=c\quad v=0$ at $y=-b\quad y=b$. The shear stress condition at $y=-a$ and $y=a$ is $\mu_1\frac{\partial u}{\partial y}=\mu_2\frac{\partial u}{\partial y}$.

Again, terms involving the ratio $\frac{\mu_2}{\mu_1}<10^{-5}$ were neglected.

In this case, the core velocity is:

$$c=Bb^2\frac{(1+\eta)}{(1-\eta)}\left\{(1-\eta)^2-\varepsilon^2\right\} \tag{2.9}$$

where ε is a dimensionless measure of the eccentricity of the core and $B=-\frac{\beta}{2\mu_2}$. Notice that $\lim_{\varepsilon\to 0}c=Bb^2(1-\eta^2)$.

Let

$$K=\frac{c}{Bb^2}=\frac{(1+\eta)}{(1-\eta)}\left\{(1-\eta)^2-\varepsilon^2\right\} \tag{2.10}$$

The total flow rate of fluid 1 is:

$$Q_1=2ac=2Bb^3\eta K \tag{2.11}$$

For the upper half, the fluid 2 flow rate Q_{2u} and average velocity V_{2u} are given by equations (2.12) and (2.13), respectively

$$Q_{2u}=\tfrac{1}{2}Bb^3\left\{(1-\eta)-\varepsilon\right\}\left\{\tfrac{1}{3}\left[(1-\eta)\left\{(1-\eta)-2\varepsilon\right\}+\varepsilon^2\right]+K\right\} \tag{2.12}$$

$$V_{2u}=\frac{Q_{2u}}{b(1-\eta)} \tag{2.13}$$

For the lower half, the fluid 2 flow rate Q_{2l} and average velocity V_{2l} are given by equations (2.14) and (2.15).

$$Q_{2l}=\tfrac{1}{2}Bb^3\left\{(1-\eta)+\varepsilon\right\}\left\{\tfrac{1}{3}\left[(1-\eta)\left\{(1-\eta)+2\varepsilon\right\}+\varepsilon^2\right]+K\right\} \tag{2.14}$$

$$V_{2l}=\frac{Q_{2l}}{b(1-\eta)} \tag{2.15}$$

Notice that $\lim_{\varepsilon\to 0}Q_{2u}=\lim_{\varepsilon\to 0}Q_{2l}=\tfrac{1}{3}Bb^3(2-3\eta+\eta^3)$.

The total flow rate of fluid 2 is:

$$Q_{2u} + Q_{2l} = \tfrac{2}{3} Bb^3 \left\{ 2 - 3\eta\left(1+\varepsilon^2\right) + \eta^3 \right\} \tag{2.16}$$

$$\lim_{\varepsilon \to 0}\left(Q_{2u} + Q_{2l}\right) = \tfrac{2}{3} Bb^3 \left(2 - 3\eta + \eta^3\right)$$

and its average velocity is:

$$V_2 = \frac{Q_{2u} + Q_{2l}}{2b(1-\eta)} \tag{2.17}$$

Then, the global holdup ratio h_g can be defined as follows:

$$h_g = \frac{c}{V_2} = \frac{3(1+\eta)\left\{(1-\eta)^2 - \varepsilon^2\right\}}{2 - 3\eta\left(1+\varepsilon^2\right) + \eta^3} \tag{2.18}$$

$$\lim_{\varepsilon \to 0} h_g = \frac{3(1-\eta)\left(1-\eta^2\right)}{2 - 3\eta + \eta^3}$$

We also can define local holdup ratios for the upper and lower halves or h_u and h_l, as follows:

$$h_u = \frac{c}{V_{2u}} = \frac{3(1+\eta)\left\{(1-\eta)^2 - \varepsilon^2\right\}}{2 - 3\eta\left(1+\varepsilon^2\right) + \eta^3 - \varepsilon(1-\eta)\left\{(1-\eta) + \varepsilon\right\}} \tag{2.19}$$

$$h_l = \frac{c}{V_{2l}} = \frac{3(1+\eta)\left\{(1-\eta)^2 - \varepsilon^2\right\}}{2 - 3\eta\left(1+\varepsilon^2\right) + \eta^3 + \varepsilon(1-\eta)\left\{(1-\eta) - \varepsilon\right\}} \tag{2.20}$$

Notice that $h_u \neq h_l \neq h_g$. However,

$$\lim_{\varepsilon \to 0} h_u = \lim_{\varepsilon \to 0} h_l = \lim_{\varepsilon \to 0} h_g = \frac{3(1-\eta)\left(1-\eta^2\right)}{2 - 3\eta + \eta^3} = h_{sym} \tag{2.21}$$

where h_{sym} corresponds to the holdup ratio for the symmetric case.

2.3 SYMMETRIC VS. ECCENTRIC 2D PERFECT CORE FLOW

Let $c_{sym} = c_{non-sym}$ or

$$\Gamma b^2\left(1-\eta^2\right) = Bb^2 \frac{(1+\eta)}{(1-\eta)}\left\{(1-\eta)^2 - \varepsilon^2\right\} \tag{2.22}$$

then

$$B = \Gamma \frac{(1-\eta)^2}{\left\{(1-\eta)^2 - \varepsilon^2\right\}}$$

where $\lim_{\varepsilon \to 0} B = \Gamma$, or

$$\beta = \gamma \frac{(1-\eta)^2}{\left\{(1-\eta)^2 - \varepsilon^2\right\}} \tag{2.23}$$

and $\lim_{\varepsilon \to 0} \beta = \gamma$

Notice that for given c, a and b; $\beta > \gamma$. The pressure drop in the non-symmetric case is higher than the pressure drop in the symmetric case. Only in the limit where $\varepsilon \to 0$ they are equal, as expected. It is worth to point out that the holdup ratio does not depend on the core's velocity c. Thus, $h_u \neq h_l \neq h_g$ for any c in the 2D non symmetric PCAF.

We can conclude that for given c, a and b, the minimum pressure drop occurs when the core is centered. Only then the global holdup ratio is equal to the local holdup ratios.

3. 2D Wavy Core Flow

Consider two eccentric immiscible fluids flowing down an infinite two dimensional horizontal pipeline; the core is occupied by fluid 1 and the annulus by fluid 2, as shown in figure 3.1.

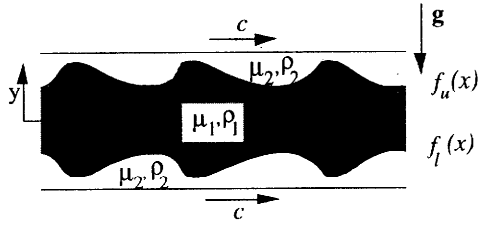

Figure 3.1. Sketch of the two dimensional wavy core flow.

Assume that fluid 1 is much more viscous than fluid 2 and there are periodic interfacial waves in upper and lower interfaces between core and annulus. According to Bai, Kelkar & Joseph [1996], the wavy core can be considered as rigid deformable body if $\frac{\mu_2}{\mu_1} < 10^{-5}$. Thus the wave speed in both interface is same as the core velocity.

3.1 PRESSURE FIELD AND GOVERNING EQUATIONS

We set up a moving frame with same core speed (see figure 3.1). We also assume that there is a connection somewhere between upper annulus and lower annuli. Thus, the pressure in the core is

$$P_1 = \beta x - \rho_1 g y + C_1 \tag{3.1.1}$$

and the pressure in both upper and lower annuli is

$$P_2 = \beta x - \rho_2 g y + p(x,y) + C_2 \tag{3.1.2}$$

The following are the governing equations for the velocity field at the indicated regions.

$$\begin{gathered}\frac{\partial u}{\partial x}+\frac{\partial v}{\partial y}=0\\ \rho_2\left(u\frac{\partial u}{\partial x}+v\frac{\partial u}{\partial y}\right)=-\beta-\frac{\partial p}{\partial x}+\mu_2\left(\frac{\partial^2 u}{\partial x^2}+\frac{\partial^2 u}{\partial y^2}\right),\\ \rho_2\left(u\frac{\partial v}{\partial x}+v\frac{\partial v}{\partial y}\right)=-\frac{\partial p}{\partial y}+\mu_2\left(\frac{\partial^2 v}{\partial x^2}+\frac{\partial^2 v}{\partial y^2}\right)\end{gathered} \tag{3.1.3}$$

in the region $-b \le y \le f_l(x)$ *and* $f_u(x) \le y \le b$,

$$\begin{gathered}u=0\\ v=0\\ \frac{dP_1}{dx}=\beta\end{gathered}$$

in the region $f_u(x) \le y \le f_l(x)$, and $u=c$ *and* $v=0$ on the boundaries or $y=\pm b$.

The general normal stress condition is

$$(-[[P]]+2H\sigma)\boldsymbol{n}+[[2\mu \boldsymbol{D}[\hat{U}]]]\bullet \boldsymbol{n}=0, \tag{3.1.4}$$

where $\hat{U}=(u,v)$, $\boldsymbol{D}[\hat{U}]=\frac{1}{2}(\nabla\hat{U}+\nabla\hat{U}^T)$, $2H$ is the sum of the principal curvatures, σ is the coefficient of interfacial tension, $\boldsymbol{n}=\boldsymbol{n}_{12}$ is the normal from liquid 1 to 2 and $[[P]]=P_1-P_2$.

According to (3.1.4) and the rigid deformable assumption, the normal stress balance at upper interface becomes

$$C_o - p(x,f_u(x))+(\rho_2-\rho_1)g f_u(x)=\sigma\left(\frac{-f_u''}{\left(1+f_u'^2\right)^{\frac{3}{2}}}\right), \tag{3.1.5}$$

and, at the lower interface

$$C_o - p(x,f_l(x))-(\rho_2-\rho_1)g f_l(x)=\sigma\left(\frac{-f_l''}{\left(1+f_l'^2\right)^{\frac{3}{2}}}\right), \tag{3.1.6}$$

where $C_o = C_1 - C_2$.

3.2 GLOBAL FORCE BALANCE

3.2.1 *Vertical direction.*

The total pressure on the wavy core in y-axis (see figure 3.2) is

$$\begin{aligned}F_{pressure}&=\int_0^{S_l}\boldsymbol{n}_l\bullet\boldsymbol{e}_y P_2(x,f_l)ds_u-\int_0^{S_u}\boldsymbol{n}_u\bullet\boldsymbol{e}_y P_2(x,f_u)ds_u\\ &=\int_0^z\left\{p_l-p_u+\rho_2 g(f_u-f_l)\right\}dx\end{aligned} \tag{3.2.1}$$

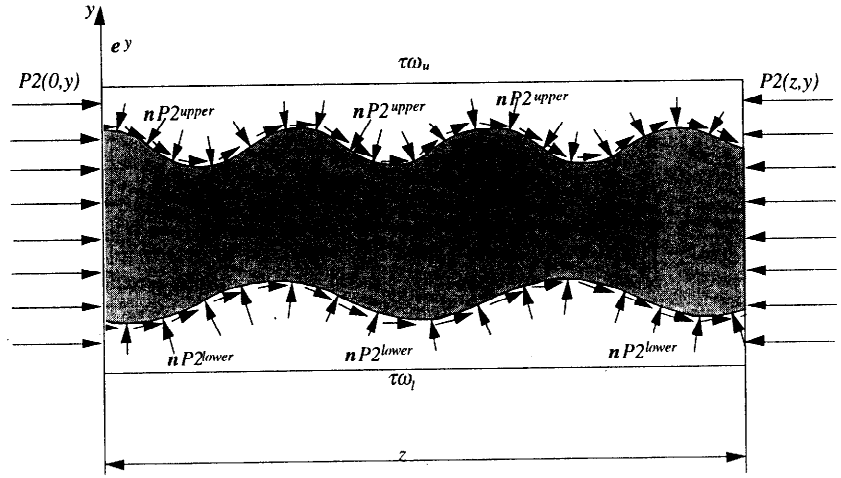

Figure 3.2. Sketch of forces acting on the core.

The total shear stress on the core in vertical direction is

$$\begin{aligned}F_{shear}&=\int_0^{S_u}\boldsymbol{t}_u\tau_u\bullet\boldsymbol{e}_y ds_u-\int_0^{S_l}\boldsymbol{t}_l\tau_l\bullet\boldsymbol{e}_y ds_l\\ &=\int_0^z\tau_u f_u'dx-\int_0^z\tau_l f_l'dx=\int_0^z(\tau_u f_u'-\tau_l f_l')dx\end{aligned} \tag{3.2.2}$$

The buoyancy force on the core is

$$F_{gravity}=-\int_0^z(f_u-f_l)\rho_l g dx. \tag{3.2.3}$$

When the core is balanced, the following condition is satisfied:

$$F_{pressure}+F_{shear}+F_{bouyancy}=0, \tag{3.2.4}$$

or

$$\int_0^z \{p_l - p_u + \rho_2 g(f_u - f_l) + (\tau_u f_u' - \tau_l f_l') - (f_u - f_l)\rho_l g\} dx = 0. \qquad (3.2.5)$$

If we choose a very large value for z, then

$$\lim_{z\to\infty} \frac{1}{z}\int_0^z \{p_l - p_u + \rho_2 g(f_u - f_l) + (\tau_u f_u' - \tau_l f_l') - (f_u - f_l)\rho_l g\} dx$$
$$= \frac{1}{L_l}\int_0^{L_l}(p_l - \tau_l f_l')dx - \frac{1}{L_u}\int_0^{L_u}(p_u - \tau_u f_u')dx + (\rho_2 - \rho_l)g\,2a = 0 \qquad (3.2.6)$$

where L_l and L_u are the wave lengths of the lower and upper interfaces, and **2a** is the core mean size or

$$2a = \overline{f_u} - \overline{f_l} = \frac{1}{L_u}\int_0^{L_u} f_u dx - \frac{1}{L_l}\int_0^{L_l} f_l dx \qquad (3.2.7)$$

Therefore the balance condition in the vertical direction is

$$\frac{1}{L_u}\int_0^{L_u}(p_u - \tau_u f_u')dx - \frac{1}{L_l}\int_0^{L_l}(p_l - \tau_l f_l')dx = (\rho_2 - \rho_l)g\,2a \qquad (3.2.8)$$

3.2.2 *Horizontal direction.*
In the x-axis, the global shear stress balance the pressure gradient as follows

$$\int_0^z \tau_{w_u} dx + \int_0^z \tau_{w_l} dx$$
$$= 2b\beta z + \int_{f_u(z)}^{D_2} p_u(y,z)dy - \int_{f_u(0)}^{D_2} p_u(y,0)dy + \int_0^{f_l(z)} p_l(y,z)dy - \int_0^{f_l(z)} p_l(y,0)dy \qquad (3.2.9)$$
$$= 2b\beta z + \Omega$$

where ***2b*** is the gap between the parallel plates and,

$$\Omega = \int_{f_u(z)}^{D_2} p_u(y,z)dy - \int_{f_u(0)}^{D_2} p_u(y,0)dy + \int_0^{f_l(z)} p_l(y,z)dy - \int_0^{f_l(z)} p_l(y,0)dy \qquad (3.2.10)$$

is bounded. Therefore,

$$\lim_{z\to\infty}\frac{1}{z}\left(\int_0^z \tau_{w_u} dx + \int_0^z \tau_{w_l} dx = 2b\beta z + \Omega\right) \text{and} \frac{1}{2b}\left(\frac{1}{L_u}\int_0^{L_u}\tau_{w_u} dx + \frac{1}{L_l}\int_0^{L_l}\tau_{w_l} dx\right) = \beta \qquad (3.2.11)$$

since $\lim_{z\to\infty}\frac{\Omega}{z} \to 0.$

4. Dimensionless variables for the 2D wavy core flow

In our formulation lengths are scaled with the mean gap size δ between the core and the wall, pressures are scaled by $\rho_2 c^2$, and velocities are scaled with the wave speed c, so

$$u = c\bar{u} \qquad (4.1)$$

$$v = c\bar{v} \qquad (4.2)$$

$$x, y, f, L = \delta\bar{x}, \delta\bar{y}, \delta\bar{f}, \delta\bar{L} \qquad (4.3)$$

where $\delta = b(1-\eta)$ and $\eta = \frac{a}{b}$.

After equation (3.2.7) η may be expressed as :

$$\eta = \frac{a}{b} = \frac{1}{2b}\left(\frac{1}{L_u}\int_0^{L_u} f_u dx - \frac{1}{L_l}\int_0^{L_l} f_l dx\right) \qquad (4.4)$$

If we split the dimensional domain (see figure 4.1) through the core's axis and change the frame of reference for the lower half as shown in figure 4.2, we can also write the following expression.

$$\frac{\eta}{1-\eta} = \frac{1}{\bar{L}}\int_0^{\bar{L}} \bar{f} d\bar{x} \qquad (4.5)$$

where $\bar{L}$ *and* $\bar{f}$ stand for and $\overline{L_u}$ *or* $\overline{L_l}$ and $\overline{f_u}$ *or* $\overline{f_l}$ respectively.

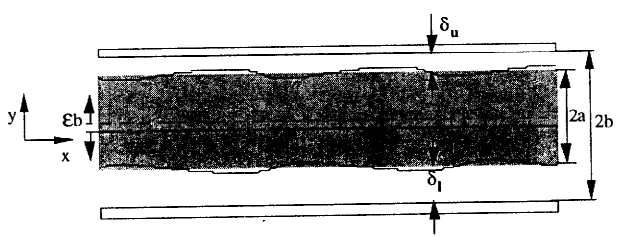

Figure 4.1 Dimensional Domain for a 2D wavy core flow.

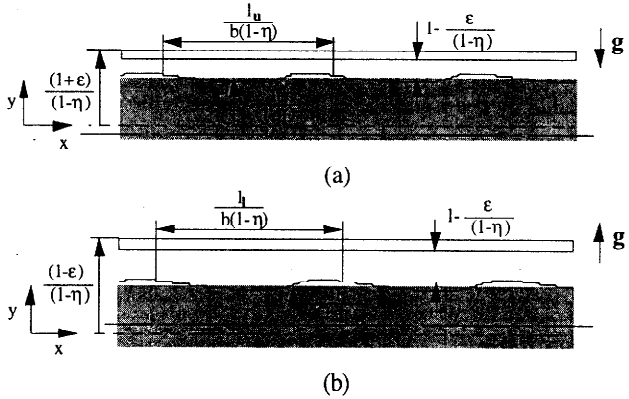

Figure 4.2 Dimensionless Domain for a 2D wavy core flow. (a) Upper half. (b) Lower half.

4.1 THE DIMENSIONLESS GOVERNING EQUATIONS

The dimensionless Navier-Stokes equations (3.1.3) are:

$$\frac{\partial \bar{u}}{\partial \bar{x}}+\frac{\partial \bar{v}}{\partial \bar{y}}=0$$

$$\left(\bar{u}\frac{\partial \bar{u}}{\partial \bar{x}}+\bar{v}\frac{\partial \bar{u}}{\partial \bar{y}}\right)=-\bar{\beta}-\frac{\partial \bar{p}}{\partial \bar{x}}+\frac{1}{\Re}\left(\frac{\partial^2 \bar{u}}{\partial \bar{x}^2}+\frac{\partial^2 \bar{u}}{\partial \bar{y}^2}\right), \tag{4.6}$$

$$\left(\bar{u}\frac{\partial \bar{v}}{\partial \bar{x}}+\bar{v}\frac{\partial \bar{v}}{\partial \bar{y}}\right)=-\frac{\partial \bar{p}}{\partial \bar{y}}+\frac{1}{\Re}\left(\frac{\partial^2 \bar{v}}{\partial \bar{x}^2}+\frac{\partial^2 \bar{v}}{\partial \bar{y}^2}\right)$$

where $\Re$ is the Reynolds number and $\bar{\beta}$ is a dimensionless pressure drop, respectively. defined as:

$$\Re=\frac{\rho_2 c b(1-\eta)}{\mu_2} \tag{4.7}$$

and

$$\bar{\beta}=\frac{b(1-\eta)}{\rho_2 c^2}\beta \tag{4.8}$$

The boundary conditions are given by (4.9) and (4.10).

$$\bar{u}=\bar{v}=0 \qquad \text{at} \qquad \bar{y}=\bar{f}_u \text{ and } \bar{y}=\bar{f}_l \tag{4.9}$$

$$\begin{matrix}\bar{v}=0\\ \bar{u}=1\end{matrix} \qquad \text{at} \qquad \bar{y}=\frac{1\pm\varepsilon}{1-\eta} \tag{4.10}$$

since the dimensionless wall speed is $\qquad \bar{c}=\frac{c}{c}=1 \tag{4.11}$

For the upper interface, the normal stress balance equation becomes

$$\bar{p}(\bar{x},\bar{f}_u)-\bar{C}_n=(1-\eta)\frac{J}{\Re^2}\left(\frac{(1-\eta)^2}{We}\bar{f}_u+\frac{\bar{f}_u''}{\left(1+\bar{f}_u'^2\right)^{3/2}}\right) \tag{4.12}$$

and for the lower interface becomes

$$\bar{C}_n-\bar{p}(\bar{x},\bar{f}_l)=(1-\eta)\frac{J}{\Re^2}\left(\frac{(1-\eta)^2}{We}\bar{f}_l-\frac{\bar{f}_l''}{\left(1+\bar{f}_l'^2\right)^{3/2}}\right) \tag{4.13}$$

where We is the Weber number, defined as:

$$We=\frac{\sigma}{(\rho_2-\rho_1)gb^2}, \tag{4.14}$$

and

$$J=\frac{\rho_2 b\sigma}{\mu_2^2} \tag{4.15}$$

Notice that $\frac{1}{We}\to 0$ as $(\rho_2-\rho_1)\to 0$; and equations (4.12) and (4.13) collapse into a single one, which corresponds to the axisymmetric case. Also notice that if $(\rho_2-\rho_1)<0$, equation (4.12) becomes equation (4.13) and vice versa, but the nature of the problem remains unchanged. For that reason, all our computations were carried out for $(\rho_2-\rho_1)>0$.

Finally, the force balance in the vertical and horizontal directions expressed by equations (3.2.8) and (3.2.11) respectively may be rewritten as:

$$\frac{1}{\bar{L}_u}\int_0^{\bar{L}_u}(\bar{p}_u-\overline{\tau_u f_u'})d\bar{x}-\frac{1}{\bar{L}_l}\int_0^{\bar{L}_l}(\bar{p}_l-\overline{\tau_l f_l'})d\bar{x}=\frac{2\eta(1-\eta)^2}{We}\frac{J}{\Re^2} \tag{4.16a}$$

$$\frac{1}{\bar{L}_u}\int_0^{\bar{L}_u}\overline{\tau_{w_u}}d\bar{x}+\frac{1}{\bar{L}_l}\int_0^{\bar{L}_l}\overline{\tau_{w_l}}d\bar{x}=2\frac{\bar{\beta}}{(1-\eta)} \tag{4.16b}$$

Therefore, only five parameters are required for a complete description of our problem: $\Re$, We, J, η and the global holdup ratio h_g which will be discussed in the next section.

4.2 THE HOLDUP RATIO

The global holdup ratio, previously defined as the ratio of the average velocities of fluid 1 and fluid 2, can be expressed as:

$$h=\frac{Q_1}{Q_2}\frac{2\delta}{2a}=c\frac{2\delta}{Q_2} \tag{4.17}$$

where Q_1 and Q_2 are the total flow rates of these fluids, δ is the mean gap size between the core and the walls and, $c = \frac{Q_1}{2a}$ is the average velocity of fluid 1.

It is easy to show that the upper and lower holdup ratios can be written as

$$h_u = c\frac{\delta_u}{Q_{2_u}}, \tag{4.18a}$$

$$h_l = c\frac{\delta_l}{Q_{2_l}}. \tag{4.18b}$$

where Q_{2u} and Q_{2l} are the fluid2 flow rates for the upper and lower halves and, δ_u and δ_l are the gap size between the core and the upper and lower walls, respectively. We also know that

$$2\delta = \delta_u + \delta_l \tag{4.19}$$

$$Q_2 = Q_{2_u} + Q_{2_l} \tag{4.20}$$

Using (4.17), (4.18a) and (4.18b), equation (4.19) can be rewritten as follows:

$$hQ_2 = h_u Q_{2_u} + h_l Q_{2_l} \tag{4.21}$$

And, the system of equations reduces to equations (4.20) and (4.21). One solution is:

$$h = h_u = h_l \tag{4.22}$$

Combining (4.17), (4.19) and (4.20), we obtain another look of the system, namely

$$\begin{aligned} h &= c\frac{\delta_u + \delta_l}{Q_{2_u} + Q_{2_l}} \\ h_u &= c\frac{\delta_u}{Q_{2_u}} \\ h_l &= c\frac{\delta_l}{Q_{2_l}} \end{aligned} \tag{4.23}$$

By inspection, we conclude that only if $h_u = h_l$, equation (4.22) holds; that is the global holdup ratio is equal to the local holdup ratio everywhere.

A more general solution is the following:

$$Q_{2_l} = \frac{h - h_u}{h_l - h_u} Q_2 \tag{4.24}$$

$$Q_{2_l} = \frac{h_l - h}{h_l - h_u} Q_2 \tag{4.25}$$

In order to keep Q_{2_u} *and* Q_{2_l} positive, we need that

$$h_l \geq h \geq h_u \quad or \quad h_u \geq h \geq h_l \tag{4.26}$$

Finally, we have to point out that the global and/or the local holdup ratios are physically restricted, thus (4.26) becomes

$$2 > h_l \geq h \geq h_u > 1 \quad or \quad 2 > h_u \geq h \geq h_l > 1 \tag{4.27}$$

The lower limit is achieved when the crests of the waves touch the wall; fluid 2 is trapped within the valleys of the interface and it travels at the same speed c. The upper limit is given for PCF when η tends to zero.

Example. Figure 4.3 shows all the possible values for the lower holdup ratio h_l as a function of the lower gap size δ_u parametrized by the upper holdup ratio h_u for $\Re$=360, η=0.76 and h=1.28. As we can see, for each upper holdup ratio h_u, the lower holdup ratio h_l may be out of bound of the region of the physical holdup ratio, except for the case of $h_l = h_u = h$.

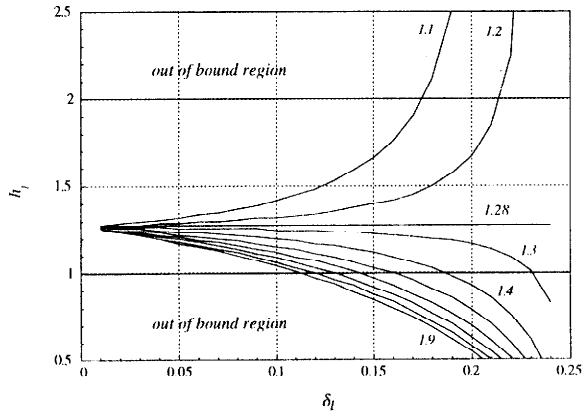

Figure 4.3. Lower holdup ratio h_l Vs. lower gap size δ_u, parametrized by the upper holdup ratio h_u for $\Re$=360, η=0.76 and h=1.28.

5. Numerical Results

Figure 5.1 presents the dimensionless pressure gradient $\overline{\beta}/(1-\eta)$ and the lower holdup ratio h_l as a function of the upper holdup ratio h_u for $\Re$=360, η=0.76, h_g=1.28, We=133 and J=1.3x10^5. It is clear that the pressure gradient is minimum when the lower and upper holdup ratios are equal, and hence, equal to the global holdup ratio or

$h_l = h_u = 1.28$. Figure 5.2 presents the eccentricity and the lower and upper wave lengths for the same case. Notice that the eccentricity also has a minimum when $h_l = h_u = 1.28$, and that the lower a upper wave length are as similar as possible. Summarizing, when the local holdup ratios are equal, the pressure gradient and the eccentricity are minimum, and the wave lengths are as close as possible, leading to a wavy core flow as symmetric (and far from the walls) as possible.

Figure 5.3 shows the dimensionless pressure gradient $\overline{\beta}$ and eccentricity ε as a function of the Reynolds number $\Re$ for η=0.80, $h_l = h_u \approx 1.29$, We=133 and J=1.3x10^5. The greater the Reynolds number, the smaller the eccentricity and the dimensionless pressure gradient $\overline{\beta}$, as we would expect, even though on dimensional grounds, the pressure gradient increases as $\Re$ increases. Figure 5.4 presents the dimensionless lower and upper wave lengths $\overline{L_1}$ and $\overline{L_2}$ as a function of the Reynolds number $\Re$ for the same case. We observe that for lower $\Re$ the upper wave length is shorter than the lower wave length, but for high $\Re$ they are almost equal.

Finally, figure 5.5 shows a sequence of cartoons that illustrate the wavy core flows corresponding to the data points that appear in figures 5.3 and 5.4. Notice how uneven the wave shapes look for the lowest Reynolds number and compare to figure 1.2, keeping in mind that this is a 3D wavy core flow. They look similar. Figures 5.3, 5.4 and 5.5 suggest that inertia helps to keep the core away from the walls and an overall flow as symmetric as possible.

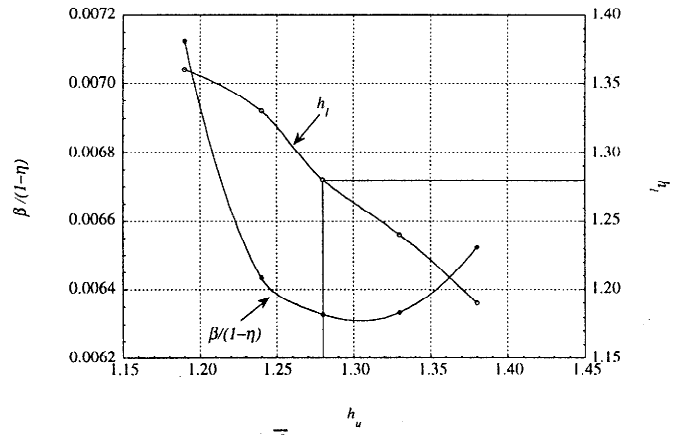

Figure 5.1. Dimensionless pressure gradient $\overline{\beta}$ and lower holdup ratio h_l as a function of the upper holdup ratio h_u, for $\Re$=360, η=0.76, h_g=1.28, We=133 and J=1.3x10^5. The smallest pressure gradient corresponds to the point of $h_l = h_u \approx 1.28$.

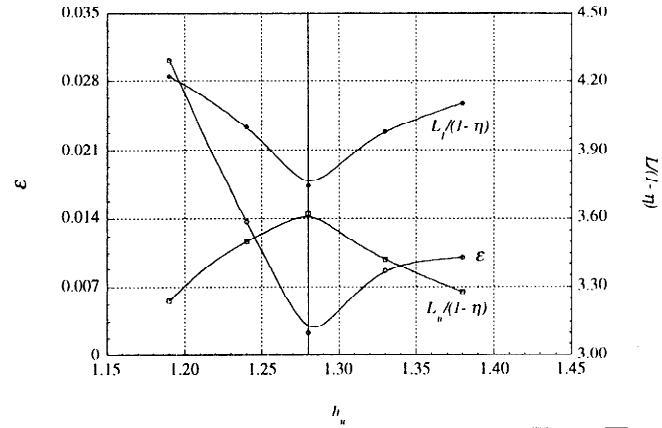

Figure 5.2. Eccentricity ε and lower and upper dimensionless wave lengths $\overline{L_l}$ and $\overline{L_u}$ as a function of upper holdup ratio h_u, for $\Re$=360, η=0.76, h_g=1.28, We=133 and J=1.3x10^5. The smallest pressure gradient corresponds to the point of $h_l = h_u \approx 1.28$.

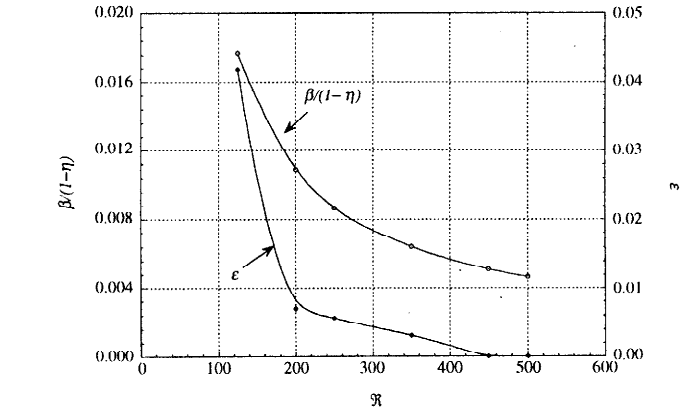

Figure 5.3. Dimensionless pressure gradient $\overline{\beta}$ and eccentricity ε as a function of the Reynolds number $\Re$, for η=0.80, $h_l = h_u \approx 1.29$, We=133 and J=1.3x10^5.

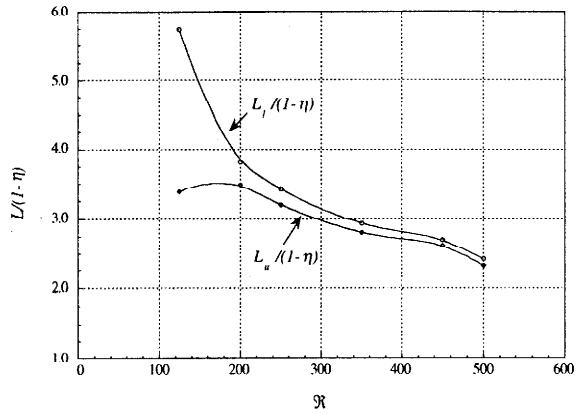

Figure 5.4. Lower and upper dimensionless wave lengths $\overline{L_l}$ and $\overline{L_u}$ as a function of Reynolds number $\Re$ for η=0.80, $h_l = h_u \approx 1.29$, We=133 and J=1.3x10^5.

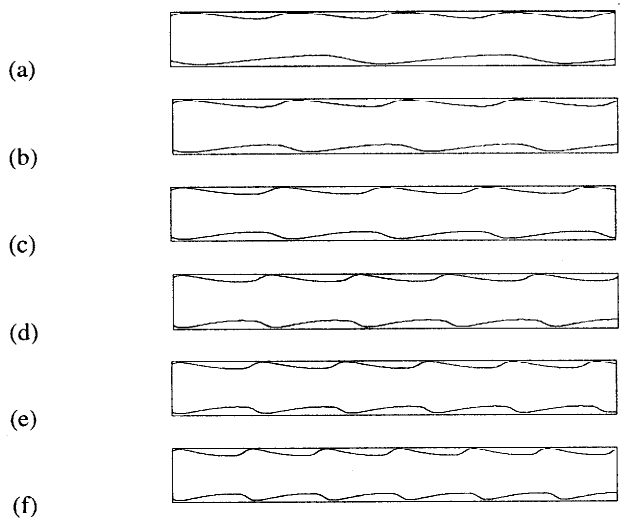

Figure 5.5. Sketch of 2D wavy core flow for increasing Reynolds numbers, η=0.80, $h_l = h_u = h_g$, We=133 and J=1.3x10^5. (a) $\Re$=125, (b) $\Re$=250, (c) $\Re$=120, (d) $\Re$=350, (e) $\Re$=450, (b) $\Re$=500.

6. Concluding remarks

Two local holdup ratios can be defined in Eccentric Perfect Core Flow (EPCF). In general, these holdup ratios are different. Only when the core is centered, they are equal and, the pressure gradient is minimum.

In 2D wavy core flows pressure gradient and eccentricity are funtion of a five-parameter set, namely $\left(\Re, We, J, \eta, h_g\right)$. Among these parameters we find the global holdup ratio. Two local holdup ratios can also be defined. When they are equal and, thus, equal to the global holdup ratio, the pressure gradient and the eccentricity are minimum. Also, there is evidence that inertia plays a role in keeping the core away from the walls.

Additional numerical work is required to completely describe the behavior of levitated core flows.

7. References

Bai, R., Kelkar, K. & Joseph, D. D. (1996) Direct simulation of interfacial waves in a high-viscosity-ratio and axisymmetric core-annular flow, *J. Fluid Mech.* **327**, 1-34.

Feng, J., Huang, P. Y., & Joseph, D. D. (1995) Dynamic simulation of the motion of capsules in pipelines, *J. Fluid Mech.* **286**, 201-227.

Joseph, D. D., & Renardy, Y. Y. (1993) *Fundamentals of two-fluid dynamics*, Springer-Verlag New York.

Oliemans, R. V. A. & Ooms, G. (1986) Core-annular flow of oil and water through a pipeline, *Multiphase Science and Technology* **2**, eds. Hewitt, G. F., Delhaye, J. M. & Zuber, N., Hemisphere Publishing Corporation.

Ooms, G., Segal, A., Van der Wees, A. J., Meerhoff, R. & Oliemans, R. V. A. (1984) A theoretical model for core-annular flow of a very viscous oil core and a water annulus through a horizontal pipe, *Int. J. Multiphase Flow* **10**, 41-60.

Patankar, S. (1980) *Numerical heat transfer and fluid flow*, eds. Minkowycz, W. & Sparrow, M., Hemisphere Publishing Corporation.

Appendix - Computational Solution of the 2D Wavy Core Flow

The two dimensional wavy core flow is governed by equations (4.4) to (4.7); the normal stress condition on the upper and lower surfaces is specified in equations (4.8) and (4.9); and the force balance on the oil core for vertical and horizontal directions is described by equations (4.14) and (4.15) respectively. For each given value of the dimensionless five-parameter set $\left(\Re, We, J, \eta, h_g\right)$, computational solution of these equations is carried out to determine the flow of water, the shape and location of the upper and lower interfaces, their wavelengths, and the eccentricity. This task is iteratively achieved in two steps. First, the computational domain is split at the center of the core; then iterative solutions of the water flow field and the interface shape are found for each half. Secondly, the net force on the vertical direction is computed and if not zero, the location of the core center is modified in order to correct it. In this step we also compute the total shear stress acting on the upper and lower walls and the pressure gradient $\overline{\beta}$ is updated. The overall solution method involves an outer iteration related to the balance of the vertical forces acting on the core and a two-step inner iteration related to the calculation of the water flow field and determination of the upper and lower interfaces. The procedure is outlined below.

1. Prescribe the wave speed c, properties of fluids 1 and 2, such as density jump (ρ_2-ρ_1), surface tension σ and viscosity μ_2, values for the core size ***2a*** and walls separation ***2b***

and the global holdup ratio h_g, which corresponds to the dimensionless five-parameter set $(\Re, We, J, \eta, h_g)$.

2. Assume the upper and lower interfaces shape. For each half of the domain, calculate the velocity and pressure fields in the water region for the specified Reynolds Number $\Re$. The Patankar's finite control volume method is used (1980). During each iteration of the flow field calculation, the pressure gradient $\overline{\beta}$ is adjusted to satisfy the force balance in the horizontal direction on the oil plug.
3. The shape of each interface is determined by solving the appropriate equation describing the normal stress condition for the interfacial pressure distribution determined in step 2. The wave length $\overline{L}$ and pressure constant $\overline{C}_o$ for each interface are adjusted in each iteration so that at convergence each interface shape is determined for the prescribed value of η and the difference between the available local holdup ratios.
4. Calculate the net vertical force and according to its sign move the location of the center of the core upwards or downwards, keeping track of the displacement.
5. The new upper and lower interfaces and the new location of the center of the core, which is a measure of the eccentricity, are used now in determining the flow field in step 2. Thus, steps 2, 3 and 4 are repeated till the vertical forces are balanced on the core. When it happens, a self-consistent flow field of water is obtained; in particular, the pressure constant $\overline{C}_o$ is the same for the lower and upper halves and the local holdup ratios are equal to the global holdup ratio. Also are obtained the shape of the upper and lower interfaces and the eccentricity of the core for the prescribed values of the five-parameter set $(\Re, We, J, \eta, h_g)$

This overall method was adapted from the one used by Bai et al [1996], which was proven to predict the same interface shape in the flow field of water irrespective of the initial guess interface. Consequently, the above method was applied for computing the details of the 2D wavy core annular flow for a range of the five-parameter set $(\Re, We, J, \eta, h_g)$.